JVI Journals.ASM.org

Rice Stripe Tenuivirus Nonstructural Protein 3 Hijacks the 26S Proteasome of the Small Brown Planthopper via Direct Interaction with Regulatory Particle Non-ATPase Subunit 3

Yi Xu,[a] Jianxiang Wu,[a] Shuai Fu,[a] Chenyang Li,[a] Zeng-Rong Zhu,[a] Xueping Zhou[a,b]

State Key Laboratory of Rice Biology, Institute of Biotechnology, Zhejiang University, Hangzhou, People's Republic of China[a]; State Key Laboratory for Biology of Plant Diseases and Insect Pests, Institute of Plant Protection, Chinese Academy of Agricultural Sciences, Beijing, People's Republic of China[b]

ABSTRACT

The ubiquitin/26S proteasome system plays a vital role in regulating host defenses against pathogens. Previous studies have highlighted different roles for the ubiquitin/26S proteasome in defense during virus infection in both mammals and plants, but their role in the vectors that transmit those viruses is still unclear. In this study, we determined that the 26S proteasome is present in the small brown planthopper (SBPH) (*Laodelphgax striatellus*) and has components similar to those in plants and mammals. There was an increase in the accumulation of *Rice stripe virus* (RSV) in the transmitting vector SBPH after disrupting the 26S proteasome, indicating that the SBPH 26S proteasome plays a role in defense against RSV infection by regulating RSV accumulation. Yeast two-hybrid analysis determined that a subunit of the 26S proteasome, named RPN3, could interact with RSV NS3. Transient overexpression of RPN3 had no effect on the RNA silencing suppressor activity of RSV NS3. However, NS3 could inhibit the ability of SBPH *rpn3* to complement an *rpn3* mutation in yeast. Our findings also indicate that the direct interaction between RPN3 and NS3 was responsible for inhibiting the complementation ability of RPN3. *In vivo*, we found an accumulation of ubiquitinated protein in SBPH tissues where the RSV titer was high, and silencing of *rpn3* resulted in malfunction of the SBPH proteasome-mediated proteolysis. Consequently, viruliferous SBPH in which RPN3 was repressed transmitted the virus more effectively as a result of higher accumulation of RSV. Our results suggest that the RSV NS3 protein is able to hijack the 26S proteasome in SBPH via a direct interaction with the RPN3 subunit to attenuate the host defense response.

IMPORTANCE

We show, for the first time, that the 26S proteasome components are present in the small brown planthopper and play a role in defense against its vectored plant virus (RSV). In turn, RSV encodes a protein that subverts the SBPH 26S proteasome via direct interaction with the 26S proteasome subunit RPN3. Our results imply that the molecular arms race observed in plant hosts can be extended to the insect vector that transmits those viruses.

Rice stripe virus (RSV), one of the most destructive pathogens of rice production, has been responsible for numerous epidemics since it was first described in Japan in 1897 (1–3). RSV is the type member of the *Tenuivirus* genus, and the viral genome consists of four single-stranded RNA segments which range in size from approximately 8.9 to 2.1 kb (4, 5). RNA 1 is negative sense and encodes a putative RNA-dependent RNA polymerase. RNAs 2, 3, and 4 are ambisense, and each contains two open reading frames (ORFs), with one on the viral RNA strand (vRNA) and the second on the viral cRNA strand (vcRNA) (6). RSV vRNA 2 encodes a membrane-associated protein that reportedly is an RNA silencing suppressor and interacts with suppressor of gene silencing 3 (SGS3) (7). vcRNA 2 encodes a glycoprotein (NSvc2) which when expressed in insect cells is displayed on the membrane surface (8). NSvc2 can also target the Golgi apparatus in plants via the COP I- and COP II-dependent secretion pathways (9). RSV vRNA 3 encodes a gene-silencing suppressor and functions through size-independent and noncooperative recognition of double-stranded RNA (dsRNA) (10, 11). The protein encoded by vcRNA 3 is the RSV nucleocapsid (NC) protein (4). vRNA 4 encodes a disease-specific protein (SP) that interacts with PsbP, an extrinsic protein associated with photosystem II in plants, to enhance virus symptoms (12). SP has also been shown to play a critical role in viral spread in the bodies of insect vectors (13). RSV vcRNA 4 encodes a virus movement protein (MP) involved in cell-to-cell movement and symptom development (14–17).

RSV is transovarially transmitted by the small brown planthopper (SBPH) in a circulative-propagative manner (5). The virus moves through the midgut, salivary gland, and ovary and is associated with amorphous or filamentous inclusions in the cytoplasm of midgut epithelial cells, salivary glands, and fat bodies (18, 19). Using 454-FLX high-throughput pyrosequencing, Zhang et al. (20) found that SBPH carries genes that play a role in regulating the innate immune systems, similar to those found in other insects, which may be involved in defense against viral infection. They also found that the viral nonstructural protein 3 (NS3) is the

Received 19 October 2014 **Accepted** 22 January 2015

Accepted manuscript posted online 4 February 2015

Citation Xu Y, Wu J, Fu S, Li C, Zhu Z-R, Zhou X. 2015. *Rice stripe tenuivirus* nonstructural protein 3 hijacks the 26S proteasome of the small brown planthopper via direct interaction with regulatory particle non-ATPase subunit 3. J Virol 89:4296–4310. doi:10.1128/JVI.03055-14.

Editor: A. Simon

Address correspondence to Xueping Zhou, zzhou@zju.edu.cn.

doi:10.1128/JVI.03055-14

most abundant transcript in viruliferous SBPH, which is supported by an independent study using real-time quantitative PCR (20, 21). It is suspected that NS3 can participate in suppressing the host immune response in both plants and the insect vector (10, 20).

The 26S proteasome is the major nonlysosomal proteolytic machinery found in eukaryotes, and it is responsible for the degradation of substrates targeted specifically by polyubiquitin modification (22, 23). The 26S proteasome has a molecular mass of about 2,000 kDa and contains one 20S protein subunit and two 19S regulatory cap subunits (24–26). The 20S core, a hollow, barrel-shaped cylinder composed of four stacked rings, has catalytic degradation activity (24). The 19S component is divided into a "base" subunit containing six ATPases (Rpt proteins) and two non-ATPases (RPN1 and RPN2) and a "lid" subunit composed of eight stoichiometric proteins (RPN3, RPN5, RPN6, RPN7, RPN8, RPN9, RPN11, and RPN12) (27). It is suspected that the 19S units perform several essential functions, including binding and unfolding specific ubiquitinated protein substrates, cleaving the attached ubiquitin (Ub) chains, opening the 20S subunit, and facilitating translocation of the unfolded polypeptide into the 20S proteolytic chamber for degradation (28, 29). RPN10 was shown to be a ubiquitin receptor, and activation of RPN11 is necessary to transfer and bind protein substrates for unfolding and translocation (30). The functions of the remaining subunits present in in the 26S proteasome are not well understood.

Several studies have demonstrated that the ubiquitin/26S proteasome system (UPS) is a critical player in the control of viral infection by targeting many viral proteins for degradation. For example, the ubiquitin-proteasome system regulates the accumulation of turnip yellow mosaic virus (TYMV) RNA-dependent RNA polymerase (RdRp) during viral infection and therefore decreases viral replication (31). Perturbation of the Ub conjugation pathway altered plant responses to tobacco mosaic virus (TMV) infection (32). TMV movement protein can be directly degraded by the host UPS in BY-2 protoplasts (33). Similarly, the TYMV MP has been shown to be a substrate for polyubiquitination, which is proposed to play a role in its degradation and enhance the ability of the host to control the transient cell-to-cell movement process (34). In turn, viruses have evolved a large number of strategies to modulate the UPS process. Virus infection can affect the transcription levels of genes important for the UPS process (35, 36). Alternatively, viruses also can modulate the UPS process by directly interacting with UPS components. For example, beet curly top virus C2 protein attenuates degradation of S-adenosylmethionine decarboxylase 1 (SAMDC1) and suppresses DNA methylation-mediated gene silencing in *Arabidopsis* (37). Adenovirus early region 1A protein regulates the 26S proteasome through direct interaction with the proteasome 19S regulatory components S4 and S8 (38). The helper component protease (HcPro) of potato virus Y can interact with three *Arabidopsis* 20S proteasome subunits (39). Ballut et al. found that lettuce mosaic virus HcPro could interact with the *Arabidopsis thaliana* α5 subunit of the 20S proteasome, and they suggested that HcPro may modulate its RNase activity, contributing to an antiviral response (40). Recently, it was found that the HcPro protein of papaya ringspot virus (PRSV) could inhibit the catalytic activity of the host proteasome and that the inhibition was achieved through interaction with the 20S proteasome subunit α1 (41). Here, we show an interaction between RSV viral protein NS3 and the insect planthopper vector's proteasome (RPN3). This interaction decreases proteasome proteolytic activity as judged by increased accumulation of ubiquitinated proteins. Together our results suggest that RSV NS3 protein subverts the SBPH 26S proteasome via direct interaction with the host RPN3 protein. Our results imply that the molecular arms race observed in plant hosts can be extended to the insect vector that transmits those viruses.

MATERIALS AND METHODS

Source of virus, host plant, and insect vector. RSV-viruliferous *Laodelphax striatellus* (the small brown planthopper) was originally provided by the Institute of Plant Protection, Jiangsu Academy of Agricultural Sciences, China, and was maintained on *Oryza sativa* cv. Wuyujing no. 3. All *O. sativa* plants and SBPH used in this study were cultured inside a growth chamber set at 26 ± 1°C with 80% relative humidity and a photoperiod of 16 h light and 8 h dark.

Plasmid construction and Y2H analysis. *ns3* was amplified from oligo(dT) reverse-transcribed cDNAs prepared from RSV-infected rice and cloned into the pGBKT7 vector as bait (Clontech, Mountain View, USA). About 30 SBPH organisms from different instars were collected, and then SBPH RNA was extracted using TRIzol reagent (Life Technologies, Grand Island, NY, USA). Next, SBPH cDNA library construction was carried out directly in yeast using SMART technology (Clontech, catalog number 634901). Yeast two-hybrid (Y2H) assays were carried out by cotransformation of *Saccharomyces cerevisiae* strain Gold with SBPH cDNA and the bait plasmid containing RSV NS3 (pGBKT7-NS3). Full-length *rpn3*, *rpn7*, and *rpn12* coding sequences were amplified using primers designed with information obtained from the SBPH transcriptome database followed by 5′ rapid amplification of cDNA ends (RACE) using the 5′ RACE system (Life Technologies) and regular PCR. RPN3 was then cloned into pGADT7 using NdeI and BamHI. The *rpn3* and *ns3* genes were separately cloned into pGEX-4T-3 and pET-30a using BamHI and XbaI restriction sites. Full-length *rpn3* from of *S. cerevisiae* was cloned using the primer pair RPN3-Y-F/RPN3-Y-R with *S. cerevisiae* genomic DNA as the template. SBPH *rpn3*, *rpn7*, and *rpn12* and yeast *rpn3* were cloned into the pGADT7 vector. Sequences of other 26S proteasome subunits were obtained by searching the SBPH transcriptome database. All sequences are available upon request. For yeast complementation studies, SBPH *rpn3* was cloned into the pRS316 vector using primers RPN3-pRS-F and RPN3-pRS-R. Ycp50 and Ycp50-RPN3 were kindly provided by Eric Bailly. Plasmids Arg-βgal, Met-βgal, and Ub-Pro-βgal were ordered from Addgene (https://www.addgene.org). All primers used in these experiments are available upon request.

GST pulldown assay. For glutathione *S*-transferase (GST) pulldown assays, equal amounts of purified proteins were mixed and adjusted to 600 μl using phosphate-buffered saline (PBS). The mixture was kept in room temperature for 1 h and then added to the GST binding columns and left for 4 h at 4°C. After 10 min of centrifugation at 1,500 × *g*, the mixed proteins were washed 5 times in washing buffer, eluted, and detected by Western blotting assays using anti-His (Sigma-Aldrich, St. Louis, MO, USA) and anti-GST (Epitomics, Burlingame, CA, USA) monoclonal antibodies together.

RNA silencing suppression activity in plants. *rpn3* and *rpn7* were amplified by PCR from the corresponding GST-RPN plasmid with primers RPN3_KpnI-F and RPN3_BamHI-R or with primers RPN7_KpnI-F and RPN7_BamHI-R. The PCR product was digested and inserted into the binary vector pBin438. Plasmid pBin438-NS3, a plasmid expressing 35SGFP, and an inverted repeated sequence of green fluorescent protein (35S-dsGFP) were constructed in our lab as described previously (10). The authenticity of all constructs was confirmed by sequencing. Plasmids were then electroporated into *A. tumefaciens* strain C58C1 with a Gene Pulser II system (Bio-Rad, Hercules, CA, USA). The method for coinfiltration assays has been described previously (10).

Insect dissections and RNA extraction. Dissection of tissues from SBPH was carried out in 1× phosphate-buffered saline (PBS) solution,

and anesthetization of SBPH was by subjecting the insects to a temperature of 4°C until immobilized. The anesthetized insects were then placed in a petri dish that was kept on ice. The tissues were then kept in RNAlater solutions (Life Technologies) during dissection. All the experiments were operated under microscopy (Olympus, Tokyo, Japan). For RNA extraction, SBPHs were collected and homogenized in TRIzol reagent (Life Technology). All samples were treated with RQ1 DNase (Promega, Madison, WI, USA) to avoid DNA contamination. The RNA served as templates for reverse transcription reactions.

Yeast complementation assay. All the constructs for yeast complementation assays were transformed into freshly prepared *S. cerevisiae rpn3* temperature-sensitive (ts) mutant strain YE101 (kindly provided by Eric Bailly) competent cells. Yeast complementation experiments were performed as described previously (42, 43).

Construction of RNA interference (RNAi) vectors and dsRNA-mediated gene silencing. dsRNA corresponding to SBPH RPN11 and RPN3 was synthesized *in vitro* using the Riboprobe System-T7 kit (Promega). dsRNA of green fluorescent protein (GFP) was also generated and used as a control. The *in vitro*-synthesized dsRNA was stained with bromophenol blue (Sigma-Aldrich) and injected into the thoraxes of ice-anesthetized third-instar viruliferous SBPH nymphs using the TransferMan NK 2 micromanipulator (Eppendorf, Hamburg, Germany). Total RNA was extracted from the injected insects at different time postinjection. Quantitative PCR was carried out on the LightCycler 480@ II using the LightCycler 480@ SYBR I Master kit (Roche Applied Science, Basel, Switzerland). PCR conditions were 95°C for 5 min followed by 48 cycles at 95°C for 10 s, 60°C for 15 s, and 72°C for 20 s. The SBPH endogenous 18S rRNA gene was used as an internal control for normalization. Northern blot analysis was conducted as described previously (44). Primers used in the quantitative reverse transcription-PCR (qRT-PCR) for validation of differentially expressed genes and detection of RPN3 expression are available upon request.

Protein extraction, Western blot analysis, and β-galactosidase (β-gal) activity assay. For extraction of SBPH total protein, we mashed SBPHs in 0.01× PBS buffer using a stamping hammer, centrifuged at 4,500 rpm for 15 min, and then discarded the pellet. The supernatant was centrifuged at 15,000 rpm to discard insect fat. For yeast protein extraction, the presence of plasmids was first confirmed by PCR, yeast cultures were grown at 37°C for 4 h, and 3 ml was collected by brief centrifugation. Proteins were extracted using YeastBuster protein extraction reagent (Merck, Darmstadt, Germany). Total protein was quantified using the bicinchoninic acid (BCA) protein assay kit (Thermo Scientific, Waltham, MA, USA). An equal volume of 2× Laemmli loading buffer (pH 6.8) (containing 1% 2-mercaptoethanol and 1% SDS) was added before boiling, and an equal concentration of protein was fractionated by 12% SDS-PAGE. Proteins in the gel were blotted onto nitrocellulose membranes. For immunological detection of ubiquitin, a rabbit antiubiquitin polyclonal antiserum (Abcam, Cambridge, United Kingdom) was used. Blotted proteins were detected using commercially available alkaline phosphatase-conjugated anti-rabbit secondary antibodies (Sigma-Aldrich) and Fast 5-bromo-4-chloro-3-indolylphosphate (BICP)–nitroblue tetrazolium (NBT) substrate (Promega). For detection of NS3, an in-house-raised polyclonal antibody was used. For enzyme-linked immunosorbent assay (ELISA), insects were used chilled at −20°C for 5 min and then mashed using a tissue grinder in 40 μl 0.01× PBS for each sample. ELISA detection was then performed as described previously (45).

For the β-galactosidase activity assay, total protein was extracted from yeast as described above and an equal amount of protein prepared in a 1.5-ml Eppendorf tube. All the samples were adjusted to a volume of 150 μl with 1× reporter lysis buffer (Promega), followed by the addition of 150 μl of 2× assay buffer to each tube, and samples were mixed by vortexing briefly. Reaction mixtures were incubated at 37°C until a faint yellow color developed. The reaction was stopped by the addition of 0.5 ml 1 M sodium carbonate. Following centrifugation, 0.9 ml of the clear supernatant was transferred to a cuvette, and absorbance was measured at 450 nm.

Planthopper (SBPH) transmission assays. Viruliferous SBPH insects reared on *O. sativa* plants were used in our transmission assays. About 100 to 200 three-instar viruliferous SBPHs were collected and injected with dsRNAs of RPN3, and the same amounts of SBPHs were injected with dsRNAs of GFP as a control. The SBPH nymphs were then transferred to healthy rice seedlings for rearing over 4 days. Ten juvenile planthoppers were then transferred per healthy rice seedling (*O. sativa* cv. Wuyujing no. 3) for a 2-day inoculation access period. Finally, the juvenile planthoppers from each rice seedlings were harvested separately. RNAs were extracted using TRIzol reagent (Life Technology) for detection of *rpn3* transcript expression, and three replicates for each treatment were conducted and three technical replicates analyzed for each biological replicate. The test rice seedlings were assayed for virus infection by RT-PCR after 1 week, 2 weeks, and 1 month.

Nucleotide sequence accession numbers. Sequences of the five full-length SBPH transcripts have been deposited in GenBank (*rpn3*, accession number KM999967; *rpn7*, accession number KM999968; *rpn12*, accession number KM999969; 20S-α*2*, accession number KM999970; 20S-β*5*, accession number KM999971).

RESULTS

The 26S proteasomes of SBPH and *Drosophila melanogaster* have similar components. Analysis of the SBPH transcriptome indicates that the SBPH may have an ubiquitin-mediated protein degradation system (20). However, no sequence information was reported, and no SBPH 26S proteasome-related genes were found on the NCBI website (data not shown). To test whether genes involved in assembly of the 26S proteasome also exist in SBPH, the amino acid sequences of the *D. melanogaster* 20S proteasome and 19S regulatory subunit genes were used to search the SBPH transcriptome database. We found all the records for the transcripts associated with the 20S proteasome and 19S regulatory subunit genes in SBPH, including five full-length copies for the related genes (*rpn3*, *rpn7*, *rpn12*, 20S-α*2*, and 20S-β*5*) (all data are available upon request). This indicates the presence of a proteasome regulatory network in SBPH and suggests that the 26S proteasome in SBPH is similar to that in *D. melanogaster*. All data are available upon request.

Disruption of the SBPH proteasome results in the increased accumulation of RSV. Previous work has shown that RNA interference (RNAi)-mediated knockdown of *rpn11* in both *Saccharomyces cerevisiae* and *D. melanogaster* leads to the accumulation of ubiquitin conjugate found in 26S proteasome substrates (46–48). Since we have identified a homologous transcript for *rpn11* in SBPH (data not shown), we tested whether SBPH *rpn11* played a similar role in regulating ubiquitin conjugate levels. Silencing of the SBPH *rpn11* gene resulted in the accumulation of high-molecular-weight ubiquitin-conjugated proteins (Fig. 1A), suggesting a defect in UPS function. We then tested whether disruption of the SBPH 26S proteasome had any effect on accumulation of RSV. Viruliferous SBPHs were injected with dsRNA of *rpn11* to silence the endogenous gene, which would lead to disruption of the SBPH proteasome. After 6 days, enzyme-linked immunosorbent assay (ELISA) and Northern blotting were separately performed to detect virus accumulation. As shown, the virus titer increased in insects where *rpn11* had been silenced as detected by ELISA using an antibody raised against RSV virions (Fig. 1B). In addition, the level of RSV genomic RNAs was also higher in insects in which *rpn11* had been silenced than in insects injected with dsGFP, used as a control (Fig. 1C). A qRT-PCR analysis demonstrated that in

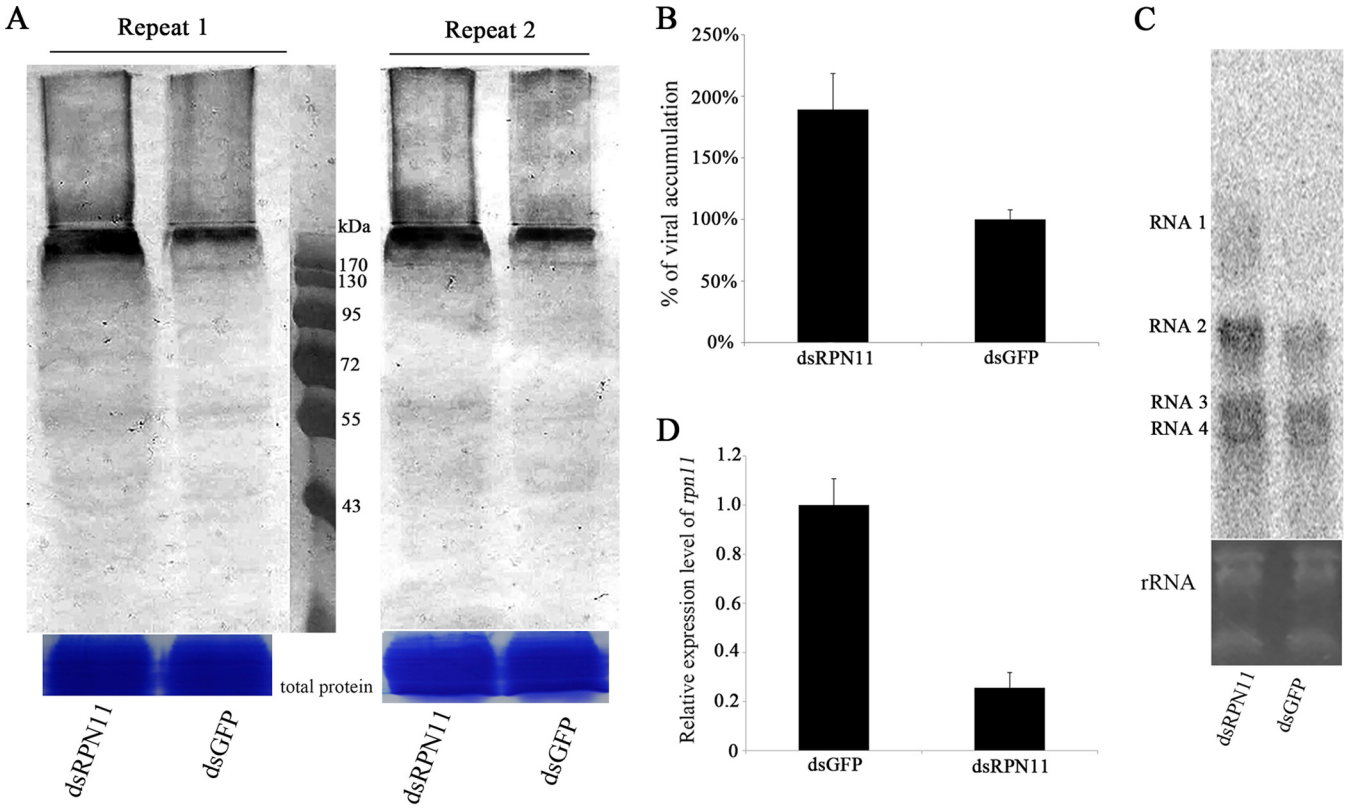

FIG 1 Ubiquitin conjugate levels and RSV accumulation increase after RNAi-mediated knockdown of *RPN11*. Six days after injection of dsRNAs of RPN11, about 20 juvenile planthoppers were used for extraction of total protein. After quantifying the protein, the same amounts of total protein were used for Western blotting and ubiquitin level detection (Fig. 1A). The RSV titer was detected using ELISA with antibody raised against RSV virions (Fig. 1B). Another 30 juvenile planthoppers from the same treatment were used for isolation of RNA for Northern blotting to detect the four RSV genomic RNAs (Fig. 1C) and for qRT-PCR for detection of the RPN11 transcript level (Fig. 1D). Three replicates for each treatment were conducted, and three technical ELISA and qRT–PCR replicates were analyzed for each biological replicate. The error bars represent standard error of the mean (SEM).

insects injected with the dsRPN11 construct, RPN11 levels were approximately 25% of those in insects injected with the control dsGFP construct (Fig. 1D). These results suggest that the SBPH UPS plays a role in the host defense response to RSV infection.

NS3 interacts with SBPH RPN3. Although the SBPH UPS appears to play a role in the host response to RSV infection, as evidenced by an increase in virus titer when a component of the 26S proteasome is silenced, the virus still survives in SBPH. We therefore sought to identify whether RSV encodes viral proteins that can suppress the host defenses. Previous work found that the transcript for the viral NS3 protein is the most abundant in viruliferous SBPH, suggesting that this protein may suppress host immune response in both plants and the insect vector (20). We therefore used this protein as bait in a Y2H assay to screen a SBPH cDNA library with the aim of identifying any host proteins that interact with NS3. From our screen we identified RPN3, which is an important component for the assembly of the 19S lid subunit in the 26S proteasome (Fig. 2A). The full-length *rpn3* coding sequence was cloned by 5′ RACE PCR and was found to be 1,497 bp long and capable of coding for a protein of 498 amino acids (data not shown). The amino acid sequence of SBPH *rpn3* is conserved in the Insecta and contains the typical proteasome component (PCI) and 26S proteasome regulatory C-terminal domains (Fig. 2B) conserved in other regulatory particle non-ATPase family proteins. To further examine the interaction between RSV NS3 and proteasome subunit RPN3 *in vitro*, His_6-tagged NS3 (HIS-NS3) and glutathione *S*-transferase-tagged RPN3 (GST-RPN3) fusion proteins were produced and purified. The *in vitro* interaction between RPN3 and NS3 was verified by pulldown assay (data not shown).

We next determined which of the RPN3 domains was responsible for the interaction with NS3 using Y2H analysis. A series of mutations in the RPN3 protein was generated and used to transform yeast strain Y2H Gold along with full-length NS3. The ability of the yeast strains to grow in synthetic dextrose dropout medium was taken as an indication of a positive interaction. As shown in Fig. 3, only yeast strains containing NS3 and a deletion of RPN3 containing amino acids 261 through 498 or amino acids 381 through 498 were able to grow. As these C-terminal fragments contain the entire 26S proteasome regulatory C-terminal domain and part of the PCI domain, it suggests that both domains may be required for the interaction with NS3. During construction of the plasmids, we obtained a mutant with a point mutation at amino acid 433, located within the 26S proteasome regulatory C-terminal domain, which changes an isoleucine to a threonine. This mutant protein lost the ability to interact with NS3, as judged by its inability to grow on synthetic dextrose dropout medium (Fig. 3). Western blotting showed that all the RPN3 mutants were expressed and remained stable in yeast cells, excluding the possibility

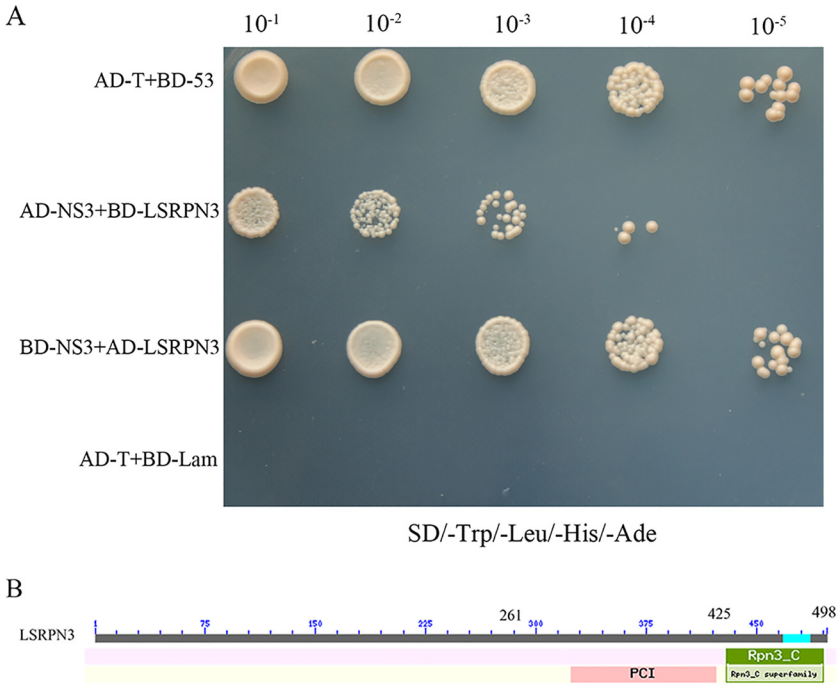

FIG 2 SBPH RPN3 and RSV-NS3 interact in a yeast two-hybrid assay. (A) Yeast strain Y2H Gold cotransformed with the indicated plasmids was spotted onto synthetic dextrose dropout medium, SD/−Trp/−Leu/−His/−Ade, in a series of 10-fold dilutions. NS3 and LSRPN3 were cloned as translational fusions with either the Gal4 activation domain (AD) or the Gal4 binding domain (BD). The mouse p53 antitumor protein (P53) and lamin C (Lam) genes were cloned as translational fusions with the Gal4 binding domain and used as positive and negative controls, respectively. (B) Schematic representation of the RPN3-coding sequence. Putative conserved functional domains of RPN3 are indicated and were deduced from InterProScan (http://www.ebi.ac.uk/Tools/InterProScan/).

that lack of interaction might be caused by instability of the interacting proteins (data not shown).

We then tested which of the NS3 domains were required for interacting with RPN3 using the same Y2H approach. Only yeast strains containing full-length RPN3 and the first 170 amino acids of NS3 were able to grow. Removal of the C-terminal 41 or N-terminal 60 amino acids resulted in a loss of growth, indicating loss of interaction with RPN3 (data not shown).

Considering that other 26S regulatory particle non-ATPase family proteins also have conserved PCI and 26S proteasome regulatory C-terminal domains (49) and that RPN7 and RPN12 have been reported to bind with RPN3 to form a multisubunit complex in *S. cerevisiae* (50), we tested whether NS3 could interact with RPN7 and RPN12 using Y2H analysis. Yeast strains containing full-length NS3 and either RPN7 or RPN12 failed to grow on synthetic dextrose dropout medium (data not shown). This indicates that the NS3 protein of RSV does not interact directly with RPN7 or RPN12, demonstrating that the interaction between NS3 and RPN3 is specific.

Expression pattern of *rpn3*. RPN3 represents one of several non-ATPase subunits in the 19S regulatory particle, but the expression pattern of this gene has never been characterized. Here, we measured steady-state levels of RPN3 mRNA in both viruliferous and nonviruliferous SBPH. Expression of RPN3 was detected in all organs of SBPH (Fig. 4A). To our surprise, the highest level of mRNA detection was found in spermary tissues, although the reason for this is unclear at this time. However, it should be noted that there is an increase in the level of RPN3 expression in this tissue in viruliferous SBPH (Fig. 4A). It is therefore possible that RSV invades the SBPH reproductive tissue, causing the increase in *rpn3* gene expression. The presence of RSV had little effect in the other tissue types, although there was a slight increase in expression levels in the head tissue (Fig. 4A). This could represent the presence of RSV in the salivary glands. Furthermore, RPN3 mRNA appears to be ubiquitously transcribed at all SBPH developmental stages (Fig. 4B). Our results show that the highest level of RPN3 expression was detectable from the fifth instar to the mature stage (Fig. 4B). However, high levels of expression were also detectable at the larval first- to second-instar stage, after which expression levels decreased.

RPN3 expression has no effect on NS3 RNA silencing suppressor activity. Plant viruses have been shown to suppress the plant RNAi pathway by producing virus-encoded RNAi suppressor proteins (RSSs). A number of approaches that involve transient expression of virus-encoded proteins in an RNAi sensor line expressing a reporter gene have been used to analyze both plant and insect viral suppressor proteins (51–53). Our previous work has documented that the RSV NS3 protein is an RSS (10). In the present study, we have used similar approaches to test NS3 suppressor activity in response to RPN3 expression. First, we cloned the *rpn3* gene into the plant binary vector pBlin438 and carried out a reversal-of-silencing assay by agroinfiltration-mediated transient ectopic expression of NS3 in *Nicotiana benthamiana* leaves. Coinfiltration of leaves with ssGFP, a dsGFP trigger, and pBlin438-NS3 showed a high level of GFP expression, indicative of the ability of NS3 to suppress the silencing of the GFP gene (Fig. 5, top panels). Coinfiltration of leaves with pBlin438-RPN3 and pBlin438-NS3 also showed a high level of GFP expression. As a control we used RPN7, which does not interact with NS3, and also observed a high level of GFP expression. These results clearly dem-

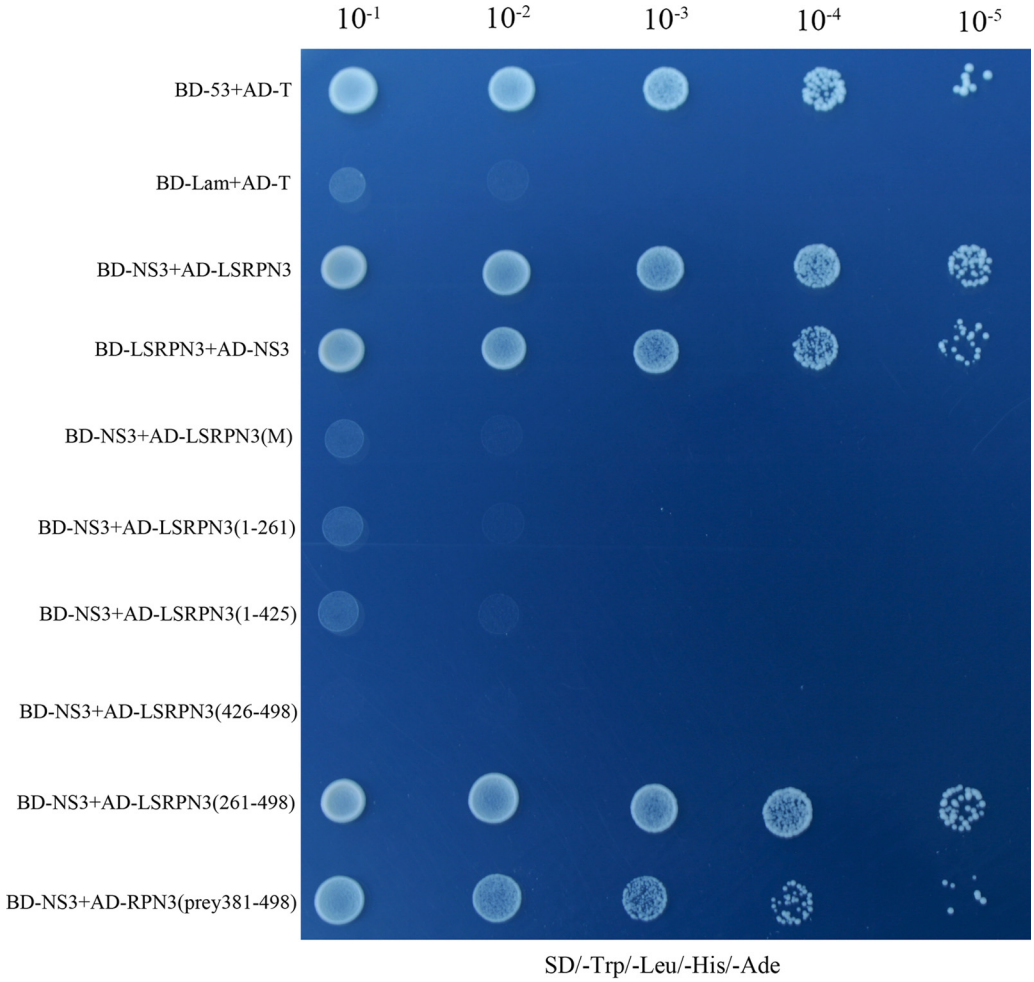

FIG 3 Identification of domains required for the interaction between RPN3 and NS3. Deletion mutants were constructed based on the conserved domains within the RPN3 protein. The deletion RPN3 (positions 1 to 261) comprises the N-terminal 261 amino acids and lacks the 26S Psome reg C and PCI domains, RPN3 (1 to 425) comprises the N-terminal 425 amino acids and contains the entire 26S Psome reg C domains, RPN3 (426 to 498) contains the entire PCI domain within amino acids 426 through 498, RPN3 (261 to 498) contains both the 26S Psome reg C and PCI domains but lacks the N-terminal 260 amino acids, RPN3 (381 to 498) is the fragment of RPN3 that we isolated as a prey plasmid in the Y2H screen, and RPN3 (M) represents a point mutation (isoleucine-to-threonine) at amino acid 433 of RPN3, within the 26S Psome reg C domain. The various mutants were cloned as translational fusions with the Gal4 activation domain (AD) and used to cotransform yeast strain Y2H Gold with full-length NS3 cloned as a translational fusion to the Gal4 binding domain. Yeast strains were spotted onto synthetic dextrose dropout medium, SD/−Trp/−Leu/−His/−Ade, in a series of 10-fold dilutions. P53 and Lam were used as positive and negative controls, respectively.

onstrate that the presence of RPN3 has no effect on the RSS activity of the RSV NS3 (Fig. 5). The expression of RPN3 and RPN7 was verified by reverse-transcription PCR (data not shown).

As a second test, we determined whether the presence of RPN3 has any effect on the ability of NS3 to suppress single-stranded RNA (ssRNA)-induced gene silencing using *N. benthamiana* 16c plants. Plasmids were individually coagroinfiltrated with plasmid p35S-ssGFP into leaves of transgenic *N. benthamiana* 16c plants as previously described (10). As can be seen in Fig. 5 (bottom panels), the presence of RPN3 or RPN7 had no effect on the ability of NS3 to suppress ssRNA-induced gene silencing.

NS3 impacts the ability of SBPH RPN3 to rescue a yeast *rpn3* mutant. In initial experiments, we tested whether SBPH RPN3 could complement the yeast temperature-sensitive (ts) *rpn3* mutant strain YE101, which is unable to form colonies when incubated on plates at 37°C (54). The ts phenotype can be fully rescued by a plasmid carrying a wild-type copy of the yeast *RPN3* gene (Ycp50-y-RPN3) (54). Expression of SBPH RPN3 restored the ability of the mutant yeast strain YE101 to grow on medium at 37°C, to levels similar to that of YE101 transformed with the yeast RPN3 (Fig. 6A). YE101 transformed with the empty expression plasmid Ycp50 failed to grow at 37°C. The RPN3 mutant containing an amino acid change at position 433 (LSRPN3-m), which is unable to bind NS3, was also able to complement the *rpn3* mutant yeast strain and grew on medium at 37°C, to levels similar to that of wild-type RPN3 (LSRPN3-wt) (Fig. 6A). Thus, SBPH *rpn3* can complement a yeast *rpn3* mutant in a complementation assay, indicating that RPN3 is a functionally conserved gene in eukaryotes. Furthermore, an *rpn3* point mutant retains the ability to complement the yeast *rpn3* mutant, demonstrating that this mutation does not impair the function of RPN3, even though it is unable to bind RSV NS3. We next asked whether the interaction

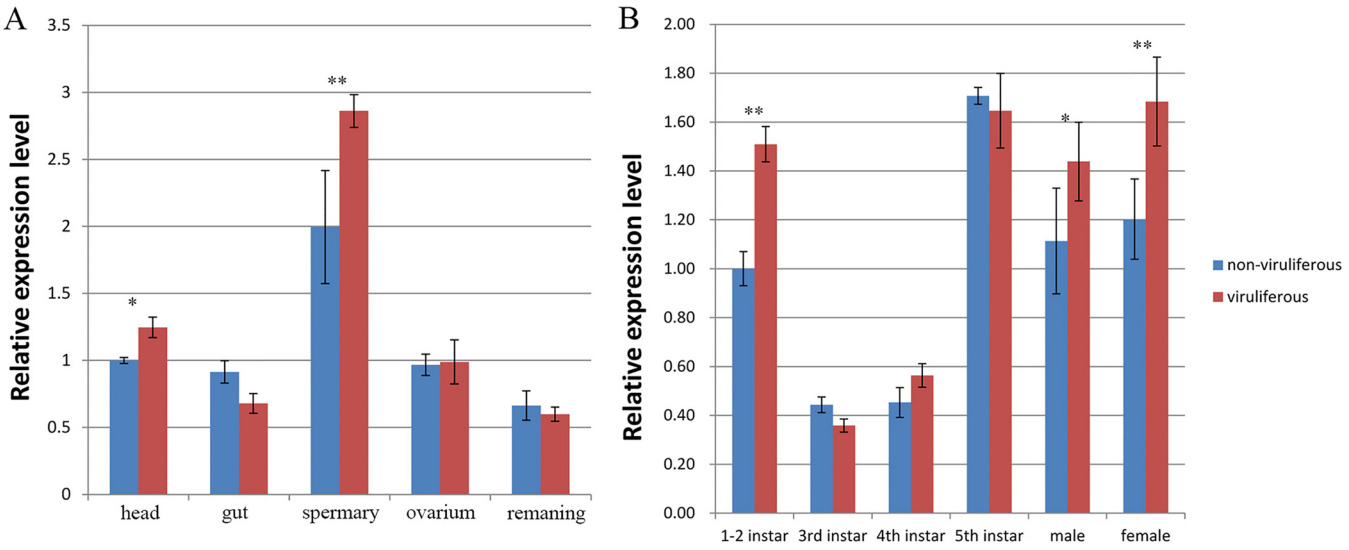

FIG 4 Characterization of the expression pattern of SBPH RPN3 mRNA. Graphs represent the expression of RPN3 mRNA in total RNA samples isolated from viruliferous and nonviruliferous planthoppers. Values were calculated by qPCR and represent the means from 3 independent replicates with standard errors of the means. Significance was assessed by one-way ANOVA on the values obtained from the different experiments (*, $P < 0.05$; **, $P < 0.01$). (A) Three-instar SBPH nymphs were dissected into head, gut (including foregut, midgut, hindgut, and Malpighian tubule), spermary, and ovarium under a stereomicroscope (Olympus). The expression level measured in the heads of nonviruliferous planthoppers was arbitrarily assigned a value of 1.00. (B) Different stages of SBPH from one- to two-instar to adult were collected, and RNA was isolated. The expression level measured at the one- to two-instar stage of nonviruliferous planthoppers was arbitrarily assigned a value of 1.00.

with NS3 could impact the ability of SBPH *rpn3* to complement the yeast *rpn3* mutant in yeast cells. As shown in Fig. 6B, YE101 cotransformed with SBPH LSRPN3-wt and NS3 exhibited limited growth at 37°C compared with YE101 transformed only with LSRPN3-wt or with LSRPN3-m. Furthermore, growth of YE101 cotransformed with SBPH LSRPN3-wt and NS3 appeared to be slower and more limited than that of yeast cotransformed with SBPH LSRPN3-m and NS3 at 37°C (Fig. 6B). To better quantify the effects of NS3 on inhibition of SBPH RPN3, we assessed growth by measuring yeast cell number over a 5-h time period. As can be seen in Fig. 6C, the mutant yeast strain transformed with empty vector (Ycp50) exhibited little growth (during the first 2 h), but yeast transformed with yeast RPN3, SBPH RPN3, or the SBPH RPN3 mutant exhibited a substantial threefold increase in cell number. Consistent with the results observed on plates, there was a decrease in cell numbers of YE101 cotransformed with SBPH LSRPN3-wt and NS3, whereas cotransformation with SBPH LSRPN3-m and NS3 had no effect on cell number (Fig. 6C). To-

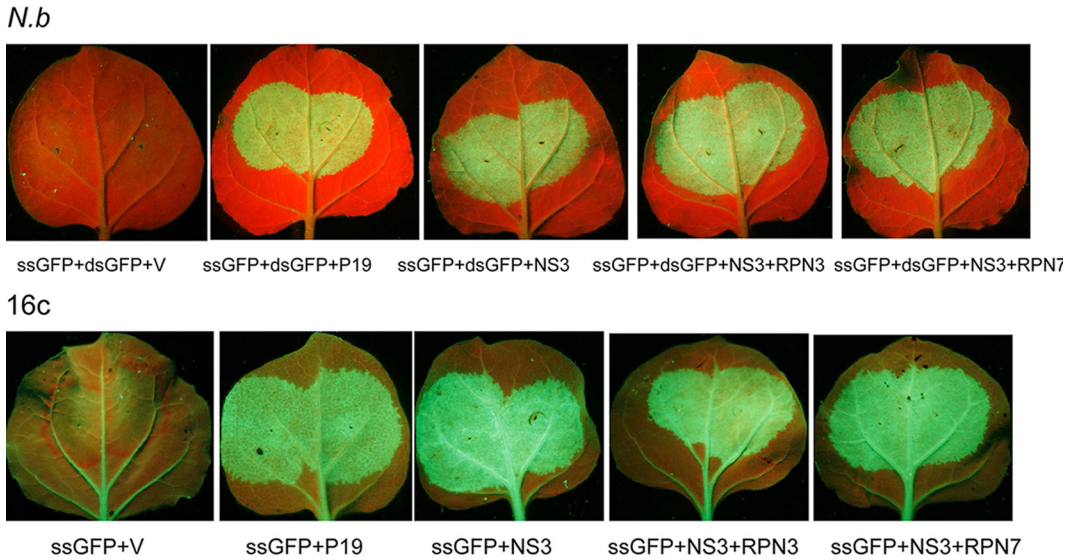

FIG 5 Expression of RPN3 has no effect on the RNA silencing suppressor activity of the RSV NS3 protein. Leaves of wild-type and transgenic GFP 16c *N. benthamiana* plants were coagroinfiltrated with a GFP-expressing vector, a vector encoding GFP-targeting dsRNA only infiltrated in *N. benthamiana*), and a vector encoding P19 (as a positive control), NS3, or NS3 with RPN3 or with RPN7. V, empty vector. The leaves were photographed at three days postinfection in *N. benthamiana* and at six days postinfection in transgenic GFP 16c plants under a hand-held long-wavelength UV illuminator (UVP, USA).

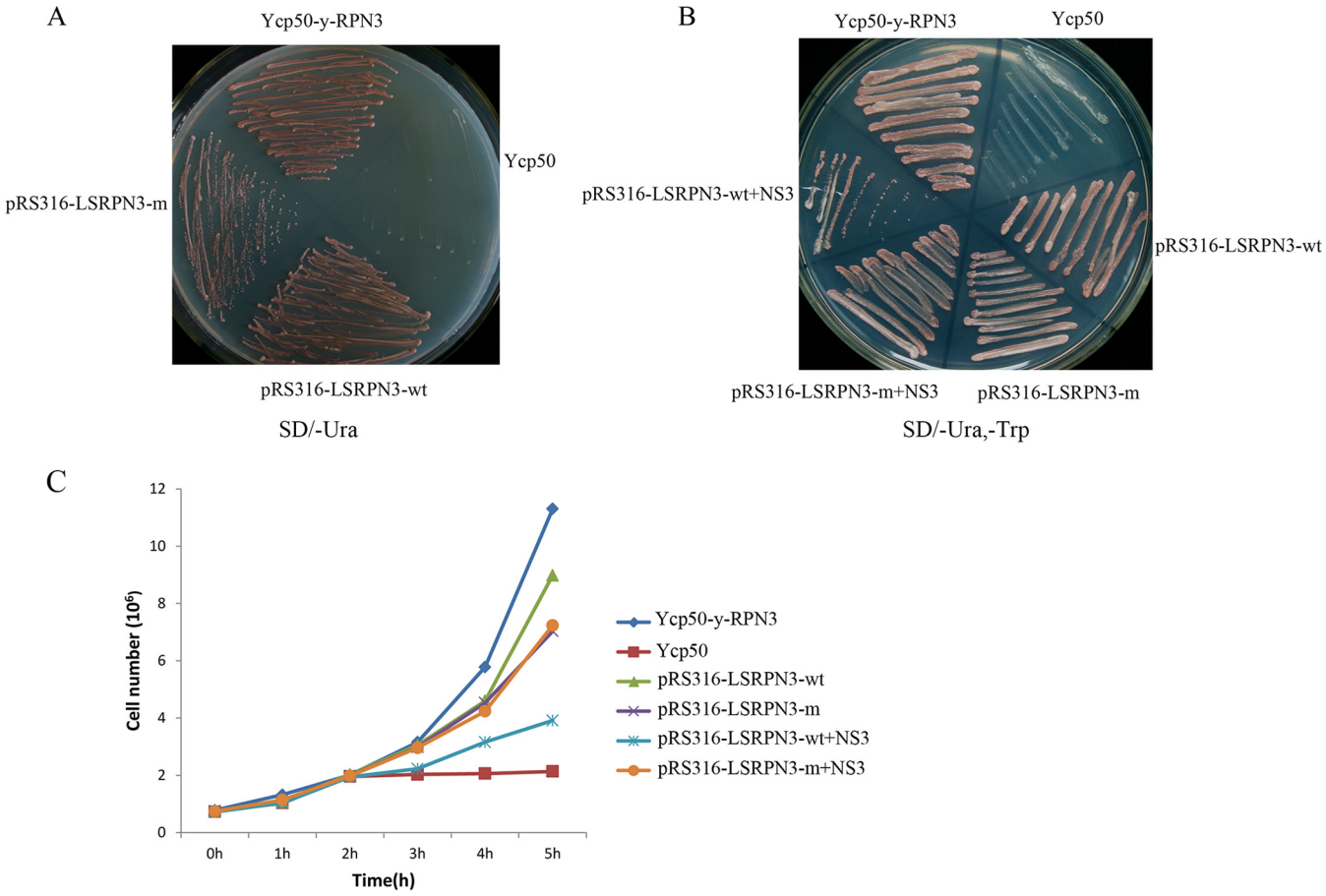

FIG 6 Coexpression of RSV NS3 inhibits the ability of SBPH RPN3 to functionally complement the yeast *rpn3* ts mutant. (A) YE101 mutant strains were transformed with SBPH RPN3 (pRS316-LSRPN3-wt) or SBPH RPN3 containing a point mutation (pRS316-LSRPN3-m), streaked on synthetic medium lacking uracil (SD/−Ura), and incubated at 37°C for 2 days. Yeast YE101 was transformed with yeast RPN3 (YCp50-y-RPN3) as a positive control and empty vector (YCp50) as a negative control. (B) YE101 mutant strains were cotransformed with either SBPH RPN3 (pRS316-LSRPN3-wt) or mutant SBPH RPN3 (pRS316-LSRPN3-m) along with pGBKT7-NS3. Yeast strain YE101 was cotransformed with empty vector (pGBKT7) and yeast RPN3 (YCp50-y-RPN3), SBPH RPN3 (pRS316-LSRPN3-wt), or the SBPH RPN3 point mutant (pRS316-LSRPN3-m) as positive controls or empty vector (YCp50) as a negative control. Plates were incubated at 37°C for 2 days. (C) Yeast YE101 transformed with the indicated plasmids was grown at 25°C to early log phase and then temperature shifted at time zero (arrow) to 37°C. At hourly intervals, cell density was measured as optical density at 600 nm, converted to cell numbers, and plotted against time.

gether, the results above suggest that NS3 can negatively affect the ability of *rpn3* to complement an *rpn3* mutant in yeast and that the inhibition is likely caused via an interaction between NS3 and RPN3.

Effects of NS3 on ubiquitin-mediated protein degradation. The *rpn3* mutant yeast strain described above (YE101), which has a temperature-sensitive growth defect, has also been shown to exhibit proteolytic defects that include the accumulation of multi-Ub proteins and stabilization of reporter substrates (54, 55). As NS3 can negatively affect the ability of *rpn3* to complement the *rpn3* ts defect in yeast (Fig. 6), we tested whether the integrity of the ubiquitin-mediated protein degradation pathway was also disrupted by NS3. In agreement with previous studies, we detected high levels of multi-Ub proteins in YE101 transformed with empty Ycp50 (Fig. 7A, lane 1) (55), consistent with a role for RPN3 in the ubiquitin-mediated protein degradation pathway. Complementation of the yeast *rpn3* mutant strain (YE101) with SBPH LSRPN3-wt or LSRPN3-m resulted in the degradation of proteolytic substrates (Fig. 7A, lanes 4 and 6), with accumulation very similar to that in YE101 transformed with yeast RPN3 (YCp50-y-RPN3) (Fig. 7A, lane 2). YE101 cotransformed with LSRPN3-wt and pGBKT7-NS3 also showed an increased accumulation of multi-Ub protein (Fig. 7A, lane 5), consistent with the ability of NS3 to inhibit the function of RPN3. In contrast, the accumulation of multi-Ub proteins was much lower in YE101 cotransformed with SBPH LSRPN3-m or yeast RPN3 (YCp50-y-RPN3) with pGBKT7-NS3 (Fig. 7A, lanes 3 and 7). This is again consistent with results that NS3 is unable to interact with the mutant RPN3 protein (Fig. 3) and that yeast RPN3 does not interact with NS3 (data not shown). These results indicate that NS3 can impair ubiquitin-mediated protein degradation in the yeast ts *rpn3* mutant complemented by SBPH *rpn3* and that the inhibition most likely occurs through a direct interaction with RPN3.

To confirm that NS3 could cause a defect in the general turnover of proteolytic substrates, we quantified degradation using both the N-end rule targeting system (Arg-βgal and Met-βgal), and the ubiquitin fusion degradation system (Ub-Pro-βgal) in yeast (56). β-Galactosidase activity was measured in triplicate using two independent preparations of protein extract (Fig. 7B, C, and D). Enzymatic activity was compared to the level detected in

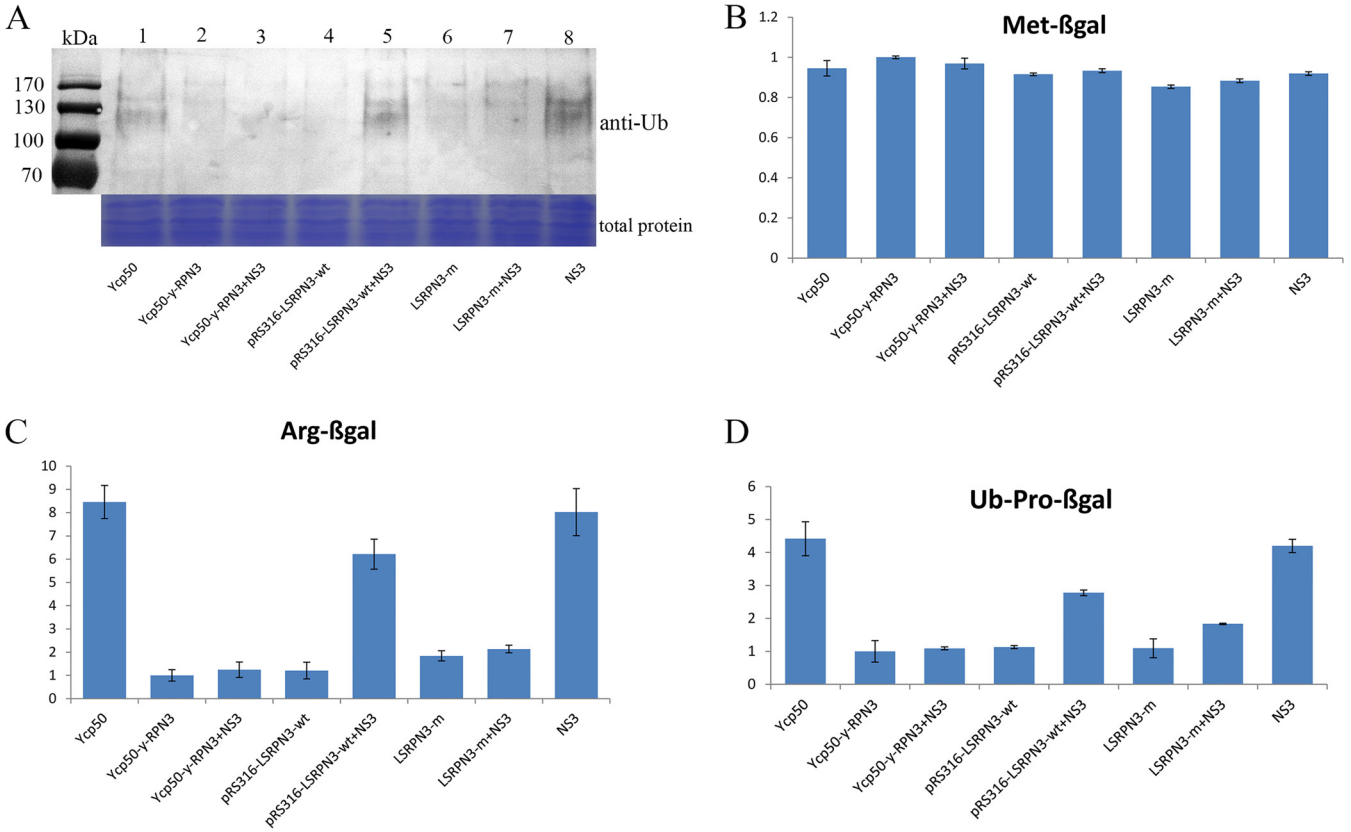

FIG 7 NS3 inhibition of SBPH RPN3 results in defective proteolysis in yeast. (A) Protein extracts were prepared from yeast transformed with the indicated plasmids (bottom). An equal amount of protein extract was resolved by SDS-PAGE and examined by immunoblotting using antibodies raised against ubiquitin. A Coomassie blue-stained SDS-polyacrylamide gel is shown below the immunoblot as a loading control. (B to D) The substrates Met-βgal, Arg-βgal, and Ub-Pro-βgal were expressed in yeast transformed with the indicated plasmids, and β-galactosidase activity was measured in triplicate. The data were quantified and standardized to expression of β-galactosidase in YE101 transformed with yeast RPN3 (Ycp50-y-RPN3). The bars represent the mean ± standard error from two independent measurements.

yeast transformed with the RPN3 positive control (Ycp50-y-RPN3), which was arbitrarily set to a value of 1. As expected, no difference in β-gal activity was detected between any of the samples using the Met-βgal assay (Fig. 7B). This was expected given that Met-βgal has a long half-life *in vivo* of >20 h (56). However, in both the Arg-βgal and Ub-Pro-βgal assays, high β-gal activity was measured in YE101 transformed with empty vector Ycp50 or only NS3 (Fig. 7C and D), indicating that overall substrate degradation is affected, leading to an increase in the amount of enzyme. When YE101 was cotransformed with wild-type yeast RPN3 (Ycp50-y-RPN3), wild-type SBPH RPN3 (LSRPN3-wt), or mutant SBPH RPN3 (LSRPN3-m), β-gal activity was reduced by 7.2 and 3.5 times in Arg-βgal and Ub-Pro-βgal assays, respectively (Fig. 7C and D), indicating that the β-gal proteolytic substrate was being degraded. Together these data are consistent with the role of RPN3 in proteolytic degradation, which is absent in the yeast *rpn3* mutant. As expected, cotransformation of YE101 with SBPH LSRPN3-wt and NS3 caused a substantial increase in β-gal activity, while β-gal activity remained low in extracts from YE101 cotransformed with NS3 and LSRPN3-m or NS3 and yeast RPN3 (Fig. 7C and D). This is again consistent with our observations that NS3 is unable to interact with the mutant RPN3 protein (Fig. 3) or with yeast RPN3. Taken together, these results indicate that the ubiquitin-mediated protein degradation pathway is impaired by NS3 in yeast.

***In vivo* accumulation of proteolytic substrates in response to RSV infection.** To test whether the UPS pathway can be affected in response to RSV infection in SBPH, total protein was extracted from whole bodies of SBPH and subsequently treated with antibodies raised against ubiquitin. There appeared to be no difference in the accumulation of proteolytic substrates between viruliferous and nonviruliferous SBPH (data not shown). Given our earlier results that demonstrated differences in the expression of RPN3 in different tissues of viruliferous and nonviruliferous SBPH (Fig. 4A), we dissected the organs and tissues where RSV particles or RSV formed inclusion bodies that accumulated to high levels (18, 19) and then extracted total proteins. As shown (Fig. 8A), all the tissues extracted from the viruliferous SBPH contained a high titer of RSV, as judged by the presence of CP and NS3. After calculating the ubiquitin signal with the Image Quant TL analysis tool (GE Company, Fairfield, CT, USA), the signal value was used for analysis of variance. Although there did not appear to be much difference in the levels of ubiquitinated protein substrates by Western blotting, the proteolytic substrates were stabilized in ovaries from viruliferous compared to nonviruliferous SBPH (Fig. 8B). Significant differences in ubiquitin levels were confirmed by one-way analysis of variance (ANOVA) ($P < 0.05$). This suggests that the ubiquitin-mediated protein degradation pathway can be impaired in SBPH after RSV infection, at least in the ovaries. Proteins extracted from the head and gut had no ob-

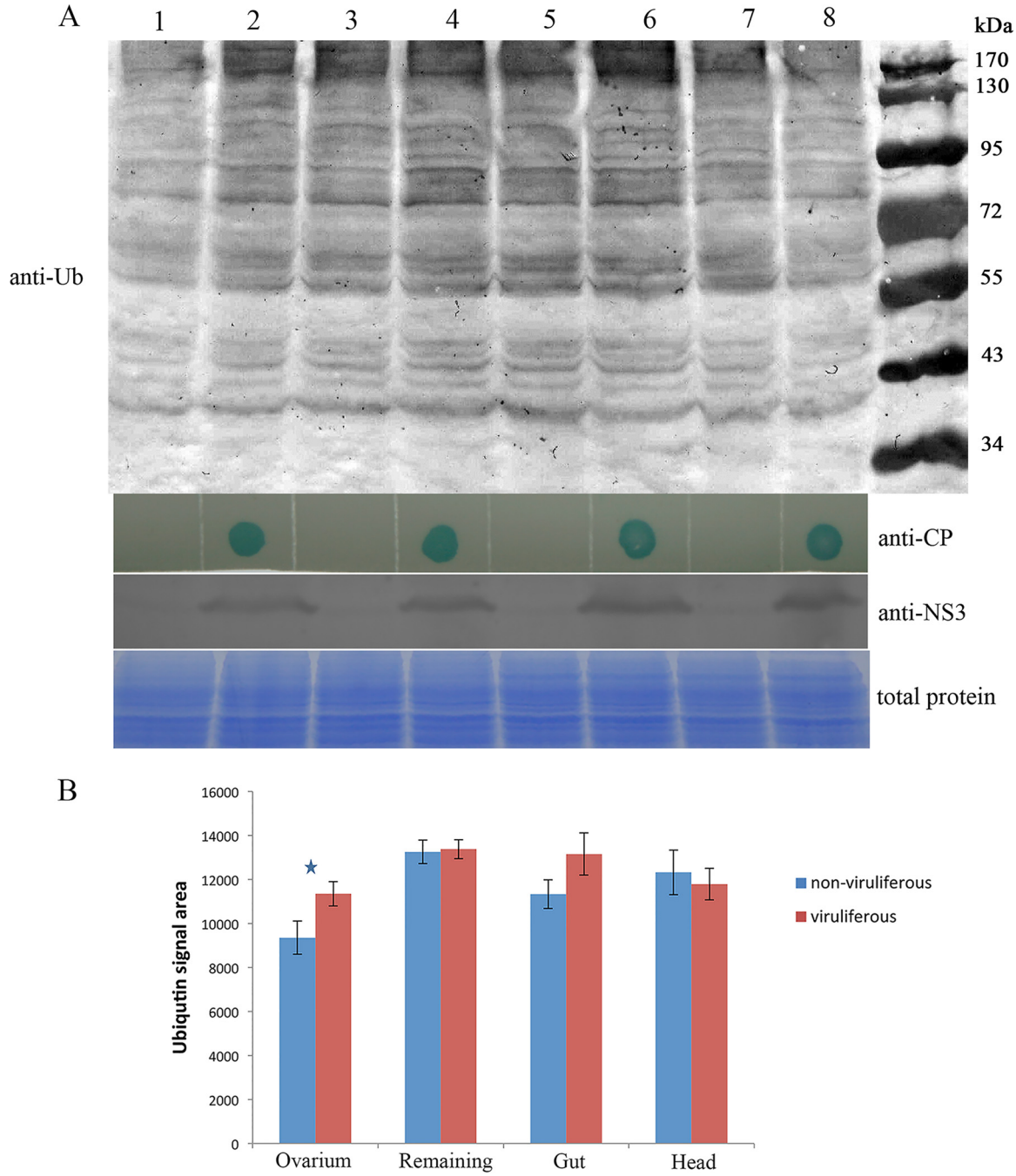

FIG 8 Ubiquitin conjugates accumulate in tissues with high levels of RSV. (A) Total proteins were extracted from different tissues, and an equal amount of protein was used for Western blot analysis. Antibodies against ubiquitin, NS3, and RSV were used to detect ubiquitinated substrates, NS3, and coat protein (CP), respectively. The lower panel represents a Coomassie blue-stained SDS-polyacrylamide gel for loading comparisons. Lanes 1, 5, and 7 represent protein extracts from the ovarium, tharm, and head, respectively, of nonviruliferous SBPH. Lane 3 represents the remaining tissues after removal of the ovarium, tharm, and head. Lanes 2, 4, 6, and 8 represent proteins extracted from the equivalent tissues of RSV-viruliferous SBPH. (B) Measurement of the ubiquitin signal was calculated using the Image Quant TL analysis tool (GE Company). We carried out three replicates for this assay. Asterisks indicate significant differences in ubiquitin levels ($P < 0.05$ by one-way ANOVA).

vious differences in the levels of ubiquitin-proteolytic substrates (Fig. 8). It is possible that the virus titer may be low in these tissues compared with that in ovaries.

Repression of RPN3 in viruliferous SBPH leads to increased accumulation of RSV and increased virus transmission. Previous work has reported that the proteasome assembly defect in *rpn3* mutants is associated with RPN11 instability and that silencing or mutation of *rpn*11 can stabilize ubiquitin pathway substrates in *Drosophila* and yeast (46, 55). Therefore, we tested whether silencing of RPN3 expression would impair UPS-mediated protein degradation in a manner similar to that observed upon silencing of RPN11. Using dsRNA injection-mediated gene

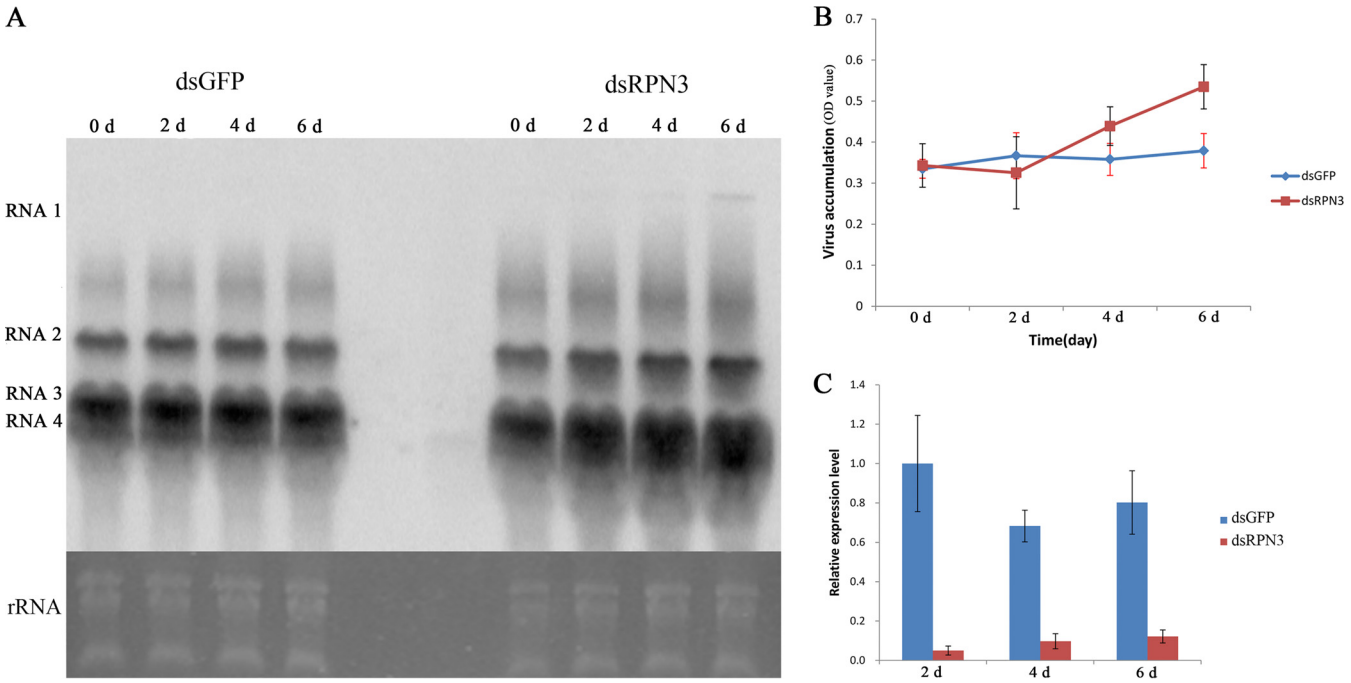

FIG 9 Silencing of SBPH RPN3 leads to increased accumulation of RSV. (A) Northern blots of total RNA isolated from viruliferous SBPH at 0, 2, 4, and 6 days after injection of dsRNA homologous to GFP or SBPH RPN3. After transfer to nylon membranes, blots were hybridized to ^{32}P-labled *in vitro* transcriptional probes specific for the RSV genome. RNA 1, 2, 3, and 4 represent four RSV segments. (B) RSV titers detected using ELISA with antibody raised against RSV virions at 0, 2, 4, and 6 days after injection of viruliferous SBPH with dsRNA homologous to GFP or SBPH RPN3. (C) qRT-PCR analysis of RPN3 mRNA in total RNA isolated from viruliferous SBPH after treatment with dsRNA homologous to GFP or SBPH RPN3.

silencing of *rpn3*, we observed accumulations of multi-Ub proteins in protein extracts from SBPH where RPN3 was repressed (6 days after microinjection of dsRNA). RPN3 mRNA was reduced to approximately 40% of the levels observed in juveniles treated with a nonspecific trigger (dsGFP) as a control (data not shown). This suggests that RPN3 also plays an important role in maintaining the functional integrity of the UPS in SBPH. This is consistent with the function played by the homologous *rpn3* gene in yeast (54).

Next, we measured RSV accumulation after silencing of *rpn3*. Significant time course accumulations of viral RNA were observed by Northern blotting in RPN3-repressed viruliferous SBPH compared with viruliferous SBPH injected with dsGFP. Large amounts of RSV RNA accumulate in viruliferous SBPH treated with both dsGFP and dsRPN3. There is a slight increase in the accumulation of RSV in insects treated with dsRPN3 at 6 days post injection (Fig. 9A). The slight increase in RSV accumulation was also verified by an independent experiment for comparison of the virus titers at 6 days postinjection of dsRNAs (data not shown). The fact that viruliferous SBPH already contains large amounts of RSV RNAs (Fig. 9A, 0 days) makes it difficult to assess whether silencing of RPN3 has a large effect on genome accumulation. However, when we assessed virus titer by ELISA, we observed similar levels of RSV in insects treated with dsGFP and dsRPN3 up to 2 days postinjection, but at 4 days postinjection, RSV levels were increasing in insects treated with dsRPN3 (Fig. 9B). By 6 days postinjection, RSV levels were about 1.5-fold higher in RPN3-silenced insects (Fig. 9B). Expression of RPN3 was decreased between 5- to 10-fold upon treatment with dsRPN3 compared to treatment with dsGFP as measured by qRT-PCR (Fig. 9C). These data suggest that silencing of the *rpn3* gene in SBPH results in an increase, albeit relatively small, in RSV accumulation.

To test the effect of increased RSV accumulation, we tested the ability of RPN3-repressed viruliferous SBPH to transmit the virus. At 4 days postinjection, viruliferous SBPH insects treated with dsRPN3 or dsGFP were transferred to healthy rice seedlings and allowed to feed for 2 days, and plants were monitored for RSV infection. A single rice plant was shown to contain RSV, as determined by RT-PCR, as early as 7 days after transmission by RPN3-repressed viruliferous SBPH (Table 1). By 14 days posttransmission, five out of eight plants that were fed on by RPN3-repressed viruliferous SBPH contained RSV, compared to a single plant fed on by viruliferous SBPH treated with dsGFP (Table 1). By 30 days posttransmission, all plants were infected regardless of whether RPN3 was silenced or not. Significance in transmission efficiency was validated through Pearson's chi-square test using the data from 14 days posttransmission, and the *P* value was found to be

TABLE 1 Transmission efficiency of viruliferous SBPH with a silenced *RPN3* gene

SBPH treatment	No. of RSV-infected rice seedlings detected by RT-PCR/total no. of rice seedlings inoculated at postinoculation day[b]:		
	7	14	30
dsGFP injection	0/8	1/8[a]	7/8
dsRPN3 injection	1/8	5/8	8/8

[a] There was a significant difference between the two treatments ($P < 0.05$) by Pearson's chi-square test.
[b] Numbers are the total plants inoculated from two independent experiments.

<0.05, indicating valid statistical significance of the virus transmission assay. These results are consistent with the higher accumulation of RSV observed in RPN3-repressed viruliferous SBPH (Fig. 9), which results in plants becoming infected in a shorter period of time. This also suggests that the host UPS pathway may play a role in host defense by reducing the overall accumulation of RSV. In a counterresponse, RSV survives in SBPH by inhibiting the UPS through the interaction of the RSV NS3 with the host RPN3.

DISCUSSION

Insect are constantly challenged by a variety of biotic and abiotic stresses and have evolved a range of sophisticated antiviral defense mechanisms, including RNA silencing, production of antimicrobial peptides, and the ubiquitination degradation pathway (35). To successfully establish a productive infection, viruses need to translate large amounts of viral proteins, which may be accompanied by misfolded and damaged host proteins. Proteasomes are protein complexes present in all eukaryotes and are part of the mechanism by which cells regulate the concentration of particular proteins and degrade misfolded proteins. In the present study, we first identified genes encoding proteins that constitute the SBPH 26S proteasome. All the genes required for assembly of the *D. melanogaster* 26S proteasome were found in the transcriptome of SBPH. Silencing of the 19S "lid" subunits RPN3 and RPN11 in SBPH resulted in an increase in the levels of ubiquitin-conjugated substrates, possibly a result of disruption of ubiquitin-mediated proteolysis. These results are consistent with previous work on the function of RPN3 and RPN11 in *Drosophila* and yeast. Furthermore, in the present study, we found that silencing of *rpn*11 and *rpn*3 has very little effect on SBPH surviving or behaving even 2 weeks after injection (data not shown). This might be caused by the RNA interference approach with dsRNA injection technology, which could just reduce the expression level and not knock out these genes. In addition, as a result of the absence of RNA-dependent RNA polymerase, SBPH may lack the mechanisms of amplification of small RNA (44), so the silencing signals could not be sustained for a long time.

Host proteasome-mediated protein proteolysis is a common strategy for degrading viral proteins and regulating virus accumulation in both plant viruses and animal viruses (31, 33, 41, 57). In plant viruses, degraded proteins include viral replication and movement proteins, which limits viral infection (34). In animal viruses, herpes simplex virus 1 protein (ICP0) is rapidly degraded early in infection by proteasome-mediated proteolysis. We hypothesize that there may be at least two pathways. Host proteasome-mediated proteolysis may degrade host factors that are required for virus replication or translation. For example, this system may downregulate host proteins that control cell cycle transition and prevent the virus from establishing an environment suitable for virus replication. Alternatively, SBPH proteasome-mediated proteolysis may directly degrade viral proteins that are necessary for virus replication or movement.

Our results suggest that proteasome-mediated proteolysis in SBPH may play a role in defense against RSV. This is supported by evidence that disrupting the SBPH 26S proteasome increases RSV accumulation, but the molecular mechanism of how SBPH proteasome-mediated proteolysis mediates defense against RSV is still unknown. In nature, RSV is transmitted mainly by SBPH, and there is a history of long-term coevolution (4, 5). Although the SBPH UPS appears to play a role in defense against RSV accumulation, the virus still survives in SBPH. We therefore asked whether RSV has evolved a corresponding counterdefense mechanism against host proteasome-mediated proteolysis. In this current study, we demonstrate that RSV NS3 interacts with SBPH RPN3, a key subunit required for assembly of the 19S lid subunit in the 26S proteasome. Using a yeast complementation assay, we showed that *rpn*3 from SBPH could complement a yeast strain containing a temperature-sensitive mutation in the *rpn*3 gene. In addition, a point mutant of RPN3 that was unable to interact with NS3 was still able to complement the yeast mutant. This demonstrates that the mutation does not impair the function of RPN3. Our results show that NS3 can impair complementation of the yeast ts *rpn*3 mutant by wild-type SBPH *rpn*3 but not by the *rpn*3 mutant that is unable to interact with NS3. Thus, it appears that a direct interaction between NS3 and RPN3 is critical for impairing proteasome-mediated proteolysis. In support of this, we also showed that proteolytic substrates in SBPH are stabilized in response to RSV infection, especially in the tissue containing RSV. The accumulation of multi-Ub proteins in whole-body extracts of viruliferous and nonviruliferous SBPH is very similar, but there was an increase in the accumulation of proteolytic substrates in RSV-enriched tissue. This suggests an impairment of the ubiquitin-proteasome system by RSV infection, which appears to depend on the levels of virus accumulation (Fig. 8). This is consistent with other studies reporting that viral proteins, especially viral gene-silencing suppressors, can induce increased accumulation of host polyubiquitinated proteins (58). Coagroinfiltration assays demonstrate that PRSV HcPro expression mimics the action of MG132 and facilitates the accumulation of ubiquitinated proteins (41). The *Polerovirus* P0, *Tobacco etch virus* HcPro, and *Carnation Italian ringspot virus* P19 protein all induce accumulation of polyubiquitin-conjugated proteins (58). In this study, we also found a small accumulation of polyubiquitin-conjugated proteins in RSV-rich tissues of SBPH. However, we were unable to quantify the virus content and NS3 accumulation in different tissues because of the difficulty in preventing contamination during dissection.

The NS3 protein of RSV has been previously reported as a gene-silencing suppressor in plants, which counters the plant gene-silencing defense system and functions in the size-independent and noncooperative recognition of dsRNA (10, 11). We therefore asked whether the interaction between NS3 and RPN3 could impair NS3 suppressor activity, but we observed no effect on the ability of NS3 to suppress silencing (Fig. 5). We could not detect a direct interaction between rice (*Oryza sativa*) RPN3 and RSV NS3 by Y2H analysis (data not shown), and possible inhibition of the 26S proteasome by a direct interaction between NS3 and a regulatory particle non-ATPase subunit (RPN3) may happen only in insects. Whether this also occurs in plant hosts needs further investigation. Our previous work found that mutation of amino acids 173 to 175 in NS3 dramatically impairs the gene-silencing activity of the protein (10, 11). In this study, we found that the N-terminal 170 amino acids of NS3 are responsible for the interaction with SBPH RPN3. Together, these findings imply that domains of the NS3 protein that mediate suppressor activity and interact with RPN3 are different. However, this remains to be confirmed.

During the cloning of SBPH *rpn3*, we identified a mutant in which an isoleucine-to-threonine change had occurred at amino acid 433. This mutant has lost the ability to interact with NS3, and given that the mutation localizes to the region between the PCI and 26S proteasome regulatory C-terminal domain, this suggests that these regions are important for binding with NS3. A number of studies have reported that proteasome subunits can be modified by phosphorylation (59), usually at serine and threonine residues (60–63). The presence of a threonine at amino acid 433 in the mutant RPN3 protein could possibly change the phosphorylation status of RPN3. This may, in turn, cause conformational changes that result in the inability to interact with NS3. As we cloned the mutant *rpn3* using RNA extracted from a number of SBPH insects, this suggests that variants of *rpn3* may exist in the natural population of SBPH. The existence of these variants could help SBPH escape the inhibition of the 26S proteasome by the RSV NS3 protein. Thus, this may be an example of the "arms race" between RSV and its transmitting vector SBPH. Our results are consistent with the coevolutionary struggle between a plant virus and its transmitting vector. RSV encodes the NS3 protein, which has evolved to inhibit host proteasome-mediated proteolysis via a direct interaction with RPN3. In turn, the vector may be evolving variants of the RPN3 protein that cannot be recognized by NS3, and therefore the host can direct proteasome-mediated proteolysis of viral proteins.

Future work will explore whether viral proteins are targets for proteasome-mediated proteolysis. This will help us better understand the interaction between plant viruses and their transmitting vectors and may open new avenues for therapeutic intervention for plant virus-induced diseases.

ACKNOWLEDGMENTS

This research was supported by the National Key Basic Research and Development Program of China (2012CB114004), the National Natural Science Foundation of China (31272015), and the Post-Doctoral Science Foundation of China (2014M551756).

We thank Wenwu Zhou from Zhejiang University for helping with the dissection of SBPH tissues, Eric Bailly from the French Institute of Health and Medical Research for providing the yeast *rpn3* temperature-sensitive mutant strain YE101, and Zhenghe Li from Zhejiang University for kindly providing the pRS316 plasmid. We also thank Stewart Gray from Cornell University and Garry Sunter from the University of Texas at San Antonio for giving advice and editing the manuscript.

REFERENCES

1. **Wei TY, Yang JG, Liao FR, Gao FL, Lu LM, Zhang XT, Li F, Wu ZJ, Lin Q Y, Xie LH, Lin HX.** 2009. Genetic diversity and population structure of *Rice stripe virus* in China. J Gen Virol **90:**1025–1034. (Erratum, **90:**1548.) http://dx.doi.org/10.1099/vir.0.006858-0..
2. **Park HM, Choi MS, Kwak DY, Lee BC, Lee J H, Kim MK, Kim YG, Shin DB, Park SK, Kim YH.** 2012. Suppression of NS3 and MP is important for the stable inheritance of RNAi-mediated *Rice stripe virus* (RSV) resistance obtained by targeting the fully complementary RSV-CP gene. Mol Cells **33:**43–51. http://dx.doi.org/10.1007/s10059-012-2185-5.
3. **Kisimoto R.** 1965. On the transovarial passage of the *Rice stripe virus* through the small brown planthopper, *Laodelphax striatelllus* Fallen, p 73–90. *In* Conference on relationships between arthropods and plant-pathogenic viruses, Tokyo, Japan.
4. **Hibino H.** 1996. Biology and epidemiology of rice viruses. Annu Rev Phytopathol **34:**249–274. http://dx.doi.org/10.1146/annurev.phyto.34.1.249.
5. **Falk BW, Tsai JH.** 1998. Biology and molecular biology of viruses in the genus *Tenuivirus*. Annu Rev Phytopathol **36:**139–163. http://dx.doi.org/10.1146/annurev.phyto.36.1.139.
6. **Ramirez BC, Haenni AL.** 1994. Molecular-biology of *Tenuiviruses*, a remarkable group of plant-viruses. J Gen Virol **75:**467–475. http://dx.doi.org/10.1099/0022-1317-75-3-467.
7. **Du ZG, Xiao DL, Wu J G, Jia DS, Yuan ZJ, Liu Y, Hu LY, Han Z, Wei TY, Lin Q Y, Wu ZJ, Xie LH.** 2011. p2 of *Rice stripe virus* (RSV) interacts with OsSGS3 and is a silencing suppressor. Mol Plant Pathol **12:**808–814. http://dx.doi.org/10.1111/j.1364-3703.2011.00716.x.
8. **Zhao SL, Dai XJ, Liang JS, Liang CY.** 2012. Surface display of *Rice stripe virus* NSvc2 and analysis of its membrane fusion activity. Virol Sinica **27:**100–108. http://dx.doi.org/10.1007/s12250-012-3237-x.
9. **Yao M, Liu XF, Li S, Xu Y, Zhou YJ, Zhou XP, Tao XR.** 2014. *Rice stripe tenuivirus* NSvc2 glycoproteins targeted to the Golgi body by the N-terminal transmembrane domain and adjacent cytosolic 24 amino acids via the COP I- and COP II-dependent secretion pathway. J Virol **88:**3223–3234. http://dx.doi.org/10.1128/JVI.03006-13.
10. **Xiong RY, Wu J X, Zhou YJ, Zhou XP.** 2009. Characterization and subcellular localization of an RNA silencing suppressor encoded by *Rice stripe tenuivirus*. Virology **387:**29–40. http://dx.doi.org/10.1016/j.virol.2009.01.045.
11. **Shen M, Xu Y, Jia R, Zhou XP, Ye KQ.** 2010. Size-independent and noncooperative recognition of dsRNA by the *Rice stripe virus* RNA silencing suppressor NS3. J Mol Biol **404:**665–679. http://dx.doi.org/10.1016/j.jmb.2010.10.007.
12. **Kong L, Wu J, Lu L, Xu Y, Zhou X.** 2014. Interaction between *Rice stripe virus* disease-specific protein and host PsbP enhances virus symptoms. Mol Plant **7:**691–708. http://dx.doi.org/10.1093/mp/sst158.
13. **Wu W, Zheng L, Chen H, Jia D, Li F, Wei T.** 2014. Nonstructural protein NS4 of *Rice stripe virus* plays a critical role in viral spread in the body of vector insects. PLoS One **9:**e88636. http://dx.doi.org/10.1371/journal.pone.0088636.
14. **Xiong RY, Wu J X, Zhou YJ, Zhou XP.** 2008. Identification of a movement protein of the *Tenuivirus Rice stripe virus*. J Virol **82:**12304–12311. http://dx.doi.org/10.1128/JVI.01696-08.
15. **Xu Y, Zhou XP.** 2012. Role of *Rice stripe virus* NSvc4 in cell-to-cell movement and symptom development in *Nicotiana benthamiana*. Front Plant Sci **3:**269. http://dx.doi.org/10.3389/fpls.2012.00269.
16. **Zhang C, Pei XW, Wang ZX, Jia SR, Guo SW, Zhang YQ, Li WM.** 2012. The Rice stripe virus pc4 functions in movement and foliar necrosis expression in *Nicotiana benthamiana*. Virology **425:**113–121. (Erratum, **436:**244, 2012.) http://dx.doi.org/10.1016/j.virol.2012.01.007.
17. **Rong L, Lu Y, Lin L, Zheng H, Yan F, Chen J.** 2014. A transmembrane domain determines the localization of *Rice stripe virus* pc4 to plasmodesmata and is essential for its function as a movement protein. Virus Res **183:**112–116. http://dx.doi.org/10.1016/j.virusres.2014.02.006.
18. **Liang D, Qu Z, Ma X, Hull R.** 2005. Detection and localization of *Rice stripe virus* gene products in vivo. Virus Genes **31:**211–221. http://dx.doi.org/10.1007/s11262-005-1798-6.
19. **Deng JH, Li S, Hong J, Ji YH, Zhou YJ.** 2013. Investigation on subcellular localization of *Rice stripe virus* in its vector small brown planthopper by electron microscopy. Virol J **10:**310. http://dx.doi.org/10.1186/1743-422X-10-310.
20. **Zhang FJ, Guo HY, Zheng HJ, Zhou T, Zhou YJ, Wang SY, Fang RX, Qian W, Chen XY.** 2010. Massively parallel pyrosequencing-based transcriptome analyses of small brown planthopper (*Laodelphax striatellus*), a vector insect transmitting *Rice stripe virus* (RSV). BMC Genomics **11:**303. http://dx.doi.org/10.1186/1471-2164-11-303.
21. **Li S, Li X, Sun L, Zhou Y.** 2012. Analysis of *Rice stripe virus* whole-gene expression in rice and in the small brown planthopper by real-time quantitative PCR. Acta Virol **56:**75–79. http://dx.doi.org/10.4149/av_2012_01_75.
22. **Hough R, Pratt G, Rechsteiner M.** 1987. Purification of two high molecular weight proteases from rabbit reticulocyte lysate. J Biol Chem **262:**8303–8313.
23. **Ciechanover A.** 2005. Early work on the ubiquitin proteasome system, an interview with Aaron Ciechanover. Cell Death Differ **12:**1167–1177. http://dx.doi.org/10.1038/sj.cdd.4401691.
24. **Finley D.** 2009. Recognition and processing of ubiquitin-protein conjugates by the proteasome. Annu Rev Biochem **78:**477–513. http://dx.doi.org/10.1146/annurev.biochem.78.081507.101607.
25. **Murata S, Yashiroda H, Tanaka K.** 2009. Molecular mechanisms of proteasome assembly. Nat Rev Mol Cell Bio **10:**104–115. http://dx.doi.org/10.1038/nrm2630.
26. **Mochida K, Tres LL, Kierszenbaum AL.** 2000. Structural features of the

26S proteasome complex isolated from rat testis and sperm tail. Mol Reprod Dev **57:**176–184. http://dx.doi.org/10.1002/1098-2795(200010)57:2<176::AID-MRD9>3.0.CO;2-O.

27. **Gillette TG, Kumar B, Thompson D, Slaughter CA, DeMartino GN.** 2008. Differential roles of the COOH termini of AAA subunits of PA700 (19 S regulator) in asymmetric assembly and activation of the 26S proteasome. J Biol Chem **283:**31813–31822. http://dx.doi.org/10.1074/jbc.M805935200.
28. **Schreiner P, Chen X, Husnjak K, Randles L, Zhang NX, Elsasser S, Finley D, Dikic I, Walters KJ, Groll M.** 2008. Ubiquitin docking at the proteasome through a novel pleckstrin-homology domain interaction. Nature **453:**548–552. http://dx.doi.org/10.1038/nature06924.
29. **Husnjak K, Elsasser S, Zhang NX, Chen X, Randles L, Shi Y, Hofmann K, Walters KJ, Finley D, Dikic I.** 2008. Proteasome subunit Rpn13 is a novel ubiquitin receptor. Nature **453:**481–488. http://dx.doi.org/10.1038/nature06926.
30. **Unverdorben P, Beck F, Sledz P, Schweitzer A, Pfeifer G, Plitzko JM, Baumeister W, Forster F.** 2014. Deep classification of a large cryo-EM dataset defines the conformational landscape of the 26S proteasome. Proc Natl Acad Sci U S A **111:**5544–5549. http://dx.doi.org/10.1073/pnas.1403409111.
31. **Camborde L, Planchais S, Tournier V, Jakubiec A, Drugeon G, Lacassagne E, Pflieger S, Chenon M, Jupin I.** 2010. The ubiquitin-proteasome system regulates the accumulation of *Turnip yellow mosaic virus* RNA-dependent RNA polymerase during viral infection. Plant Cell **22:**3142–3152. http://dx.doi.org/10.1105/tpc.109.072090.
32. **Becker F, Buschfeld E, Schell J, Bachmair A.** 1993. Altered response to viral-infection by tobacco plants perturbed in ubiquitin system. Plant J **3:**875–881. http://dx.doi.org/10.1046/j.1365-313X.1993.03060875.x, http://dx.doi.org/10.1111/j.1365-313X.1993.00875.x.
33. **Reichel C, Beachy RN.** 2000. Degradation of *Tobacco mosaic virus* movement protein by the 26S proteasome. J Virol **74:**3330–3337. http://dx.doi.org/10.1128/JVI.74.7.3330-3337.2000.
34. **Drugeon G, Jupin I.** 2002. Stability in vitro of the 69K movement protein of *Turnip yellow mosaic virus* is regulated by the ubiquitin-mediated proteasome pathway. J Gen Virol **83:**3187–3197. http://vir.sgmjournals.org/content/83/12/3187.full.pdf+html.
35. **Wang XW, Luan JB, Li J M, Bao YY, Zhang CX, Liu SS.** 2010. De novo characterization of a whitefly transcriptome and analysis of its gene expression during development. Bmc Genomics **11:**400. http://dx.doi.org/10.1186/1471-2164-11-400.
36. **Xu Y, Zhou WW, Zhou YJ, Wu J X, Zhou XP.** 2012. Transcriptome and comparative gene expression analysis of *Sogatella furcifera* (Horvath) in response to *Southern rice black-streaked dwarf virus*. PLoS One **7:**e36238. http://dx.doi.org/10.1371/journal.pone.0036238.
37. **Zhang Z, Chen H, Huang X, Xia R, Zhao Q, Lai J, Teng K, Li Y, Liang L, Du Q, Zhou X, Guo H, Xie Q.** 2011. BSCTV C2 attenuates the degradation of SAMDC1 to suppress DNA methylation-mediated gene silencing in Arabidopsis. Plant Cell **23:**273–288. http://dx.doi.org/10.1105/tpc.110.081695.
38. **Grand RJ, Turnell AS, Mason GG, Wang W, Milner AE, Mymryk JS, Rookes SM, Rivett AJ, Gallimore PH.** 1999. Adenovirus early region 1A protein binds to mammalian SUG1-a regulatory component of the proteasome. Oncogene **18:**449–458. http://dx.doi.org/10.1038/sj.onc.1202304.
39. **Jin YS, Ma DY, Dong JL, Jin J C, Li DF, Deng CW, Wang T.** 2007. HC-Pro protein of *Potato virus Y* can interact with three Arabidopsis 20S proteasome subunits in planta. J Virol **81:**12881–12888. http://dx.doi.org/10.1128/JVI.00913-07.
40. **Ballut L, Drucker M, Pugniere M, Cambon F, Blanc S, Roquet F, Candresse T, Schmid HP, Nicolas P, Le Gall O, Badaoui S.** 2005. HcPro, a multifunctional protein encoded by a plant RNA virus, targets the 20S proteasome and affects its enzymic activities. J Gen Virol **86:**2595–2603. http://dx.doi.org/10.1099/vir.0.81107-0.
41. **Sahana N, Kaur H, Basavaraj Tena F, Jain RK, Palukaitis P, Canto T, Praveen S.** 2012. Inhibition of the host proteasome facilitates papaya ringspot virus accumulation and proteosomal catalytic activity is modulated by viral factor HcPro. PLoS One **7:**e52546. http://dx.doi.org/10.1371/journal.pone.0052546.
42. **Shen W, Hanley-Bowdoin L.** 2006. Geminivirus infection up-regulates the expression of two Arabidopsis protein kinases related to yeast SNF1- and mammalian AMPK-activating kinases. Plant Physiol **142:**1642–1655. http://dx.doi.org/10.1104/pp.106.088476.
43. **Shen Q, Liu Z, Song F, Xie Q, Hanley-Bowdoin L, Zhou X.** 2011. Tomato SlSnRK1 protein interacts with and phosphorylates betaC1, a pathogenesis protein encoded by a geminivirus beta-satellite. Plant Physiol **157:**1394–1406. http://dx.doi.org/10.1104/pp.111.184648.
44. **Xu Y, Huang L, Fu S, Wu J, Zhou X.** 2012. Population diversity of *Rice stripe virus*-derived siRNAs in three different hosts and RNAi-based antiviral immunity in *Laodelphgax striatellus*. PLoS One **7:**e46238. http://dx.doi.org/10.1371/journal.pone.0046238.
45. **Wu J, Ni Y, Liu H, Ding M, Zhou X.** 2014. Monoclonal antibody-based serological assays and immunocapture-RT-PCR for detecting *Rice dwarf virus* in field rice plants and leafhopper vectors. J Virol Methods **195:**134–140. http://dx.doi.org/10.1016/j.jviromet.2013.09.013.
46. **Verma R, Aravind L, Oania R, McDonald WH, Yates JR, III, Koonin EV, Deshaies RJ.** 2002. Role of Rpn11 metalloprotease in deubiquitination and degradation by the 26S proteasome. Science **298:**611–615. http://dx.doi.org/10.1126/science.1075898.
47. **Saunier R, Esposito M, Dassa EP, Delahodde A.** 2013. Integrity of the *Saccharomyces cerevisiae* Rpn11 protein is critical for formation of proteasome storage granules (PSG) and survival in stationary phase. PLoS One **8:**e70357. http://dx.doi.org/10.1371/journal.pone.0070357.
48. **Lundgren J, Masson P, Mirzaei Z, Young P.** 2005. Identification and characterization of a *Drosophila* proteasome regulatory network. Mol Cell Biol **25:**4662–4675. http://dx.doi.org/10.1128/MCB.25.11.4662-4675.2005.
49. **Finley D, Tanaka K, Mann C, Feldmann H, Hochstrasser M, Vierstra R, Johnston S, Hampton R, Haber J, McCusker J, Silver P, Frontali L, Thorsness P, Varshavsky A, Byers B, Madura K, Reed SI, Wolf D, Jentsch S, Sommer T, Baumeister W, Goldberg A, Fried V, Rubin DM, Toh-e A, et al.** 1998. Unified nomenclature for subunits of the *Saccharomyces cerevisiae* proteasome regulatory particle. Trends Biochem Sci **23:**244–245. http://dx.doi.org/10.1016/S0968-0004(98)01222-5.
50. **Sharon M, Taverner T, Ambroggio XI, Deshaies RJ, Robinson CV.** 2006. Structural organization of the 19S proteasome lid: insights from MS of intact complexes. PLoS Biol **4:**e267. http://dx.doi.org/10.1371/journal.pbio.0040267.
51. **Anandalakshmi R, Pruss GJ, Ge X, Marathe R, Mallory AC, Smith TH, Vance VB.** 1998. A viral suppressor of gene silencing in plants. Proc Natl Acad Sci U S A **95:**13079–13084. http://dx.doi.org/10.1073/pnas.95.22.13079.
52. **Li WX, Ding SW.** 2001. Viral suppressors of RNA silencing. Current Opin Biotechnol **12:**150–154. http://dx.doi.org/10.1016/S0958-1669(00)00190-7.
53. **Schnettler E, Sterken MG, Leung JY, Metz SW, Geertsema C, Goldbach RW, Vlak JM, Kohl A, Khromykh AA, Pijlman GP.** 2012. Noncoding *Flavivirus* RNA displays RNA interference suppressor activity in insect and mammalian cells. J Virol **86:**13486–13500. http://dx.doi.org/10.1128/JVI.01104-12.
54. **Bailly E, Reed SI.** 1999. Functional characterization of *rpn3* uncovers a distinct 19S proteasomal subunit requirement for ubiquitin-dependent proteolysis of cell cycle regulatory proteins in budding yeast. Mol Cell Biol **19:**6872–6890.
55. **Joshi KK, Chen L, Torres N, Tournier V, Madura K.** 2011. A proteasome assembly defect in rpn3 mutants is associated with Rpn11 instability and increased sensitivity to stress. J Mol Biol **410:**383–399. http://dx.doi.org/10.1016/j.jmb.2011.05.005.
56. **Bachmair A, Finley D, Varshavsky A.** 1986. In vivo half-life of a protein is a function of its amino-terminal residue. Science **234:**179–186. http://dx.doi.org/10.1126/science.3018930.
57. **Zhu Z, Du T, Zhou G, Roizman B.** 2014. The stability of HSV-1 ICP0 early after infection is defined by the RING finger and the UL13 protein kinase. J Virol **88:**5437–43. http://dx.doi.org/10.1128/JVI.00542-14.
58. **Csorba T, Lozsa R, Hutvagner G, Burgyan J.** 2010. Polerovirus protein P0 prevents the assembly of small RNA-containing RISC complexes and leads to degradation of ARGONAUTE1. Plant J **62:**463–472. http://dx.doi.org/10.1111/j.1365-313X.2010.04163.x.
59. **Barford D, Das AK, Egloff MP.** 1998. The structure and mechanism of protein phosphatases: insights into catalysis and regulation. Annu Rev Biophys Biom **27:**133–164. http://dx.doi.org/10.1146/annurev.biophys.27.1.133.
60. **Guo X, Engel JL, Xiao JY, Tagliabracci VS, Wang XR, Huang L, Dixon JE.** 2011. UBLCP1 is a 26S proteasome phosphatase that regulates nuclear proteasome activity. Proc Natl Acad Sci U S A **108:**18649–18654. http://dx.doi.org/10.1073/pnas.1113170108.

61. **Ludemann R, Lerea KM, Etlinger JD.** 1993. Copurification of casein kinase-Ii with 20S-proteasomes and phosphorylation of a 30 Kda proteasome subunit. FASEB J **7:**A1187–A1187.
62. **Bose S, Stratford FLL, Broadfoot KI, Mason GGF, Rivett AJ.** 2004. Phosphorylation of 20S proteasome alpha subunit C8 (alpha 7) stabilizes the 26S proteasome and plays a role in the regulation of proteasome complexes by gamma-interferon. Biochem J **378:**177–184. http://dx.doi.org/10.1042/BJ20031122.
63. **Satoh K, Sasajima H, Nyoumura K, Yokosawa K, Sawada H.** 2001. Assembly of the 26S proteasome is regulated by phosphorylation of the p45/Rpt6 ATPase subunit. Biochemistry **40:**314–319. http://dx.doi.org/10.1021/bi001815n.